Multiband superconductivity in $PrPt_4Ge_{12}$ single crystals

J. L. Zhang,[1] Y. Chen,[1] L. Jiao,[1] R. Gumeniuk,[2] M. Nicklas,[2] Y. H. Chen,[1] L. Yang,[1] B. H. Fu,[1] W. Schnelle,[2] H. Rosner,[2] A. Leithe-Jasper,[2] Y. Grin,[2] F. Steglich,[2] and H. Q. Yuan[1,*]

[1]*Department of Physics and Center for Correlated Matter, Zhejiang University, Hangzhou, Zhejiang 310027, China*

[2]*Max-Planck-Institut für Chemische Physik fester Stoffe, Nöthnitzer Straße 40, 01187 Dresden, Germany*

(Received 31 October 2012; published 5 February 2013)

We report measurements of the London penetration depth $\Delta\lambda(T)$ and the electronic specific heat $C_e(T)$ on high-quality single crystals of the filled skutterudite superconductor $PrPt_4Ge_{12}$ ($T_c \simeq 8$ K). Both quantities show a weak temperature dependence at $T \ll T_c$, following $\Delta\lambda \sim T^n$ ($n = 3.2 \pm 0.1$) and $C_e/T \sim T^{2.8}$. Such temperature dependences deviate from both conventional s-wave-type and nodal superconductivity. A detailed analysis indicates that the superfluid density $\rho_s(T)$, derived from the penetration depth, as well as the electronic specific heat can be consistently described in terms of a two-gap model, providing strong evidence of multiband superconductivity for $PrPt_4Ge_{12}$.

DOI: 10.1103/PhysRevB.87.064502 PACS number(s): 74.70.Tx, 74.20.Rp, 74.25.Bt, 74.70.Dd

I. INTRODUCTION

The filled-skutterudite compounds MT_4X_{12} (M = rare-earth or alkaline-earth metals, T = Fe, Ru, Os, and X = P, As, Sb) demonstrate remarkably rich physical properties.[1] Particular attention has been paid to superconductivity (SC) observed in the Pr-based compounds. For example, $PrOs_4Sb_{12}$ is a heavy-fermion superconductor with $T_c = 1.85$ K.[2] Electric quadrupole, rather than magnetic dipole, fluctuations are believed to mediate the Cooper pairs in this compound, which is unique among heavy-fermion superconductors. The superconducting order parameter of $PrOs_4Sb_{12}$ remains controversial: nodal SC[3,4] as well as s-wave SC[5] were proposed. More recent experiments seem to support a scenario of multiband SC.[6,7] On the other hand, the isostructural compounds $PrRu_4Sb_{12}$ and $PrRu_4As_{12}$ appear to be s-wave superconductors.[8,9]

Recently, a series of new skutterudite superconductors with a germanium-platinum framework, i.e., MPt_4Ge_{12} (M = Sr, Ba, La, Pr), were successfully synthesized.[10,11] Among all the Pr-filled variants, $PrPt_4Ge_{12}$ shows an unexpectedly high transition temperature of $T_c = 7.9$ K.[11] The Sommerfeld coefficient of $PrPt_4Ge_{12}$ ($\gamma_n = 76$ mJ/mol K^2)[12] is comparable to that of $PrRu_4Sb_{12}$ (Ref. 8) and $PrRu_4As_{12}$ (Ref. 9) but much smaller than that of $PrOs_4Sb_{12}$.[2] Furthermore, the crystalline electric field (CEF) splitting of the $J = 4$ Hund's rule multiplet of Pr^{3+} between the Γ_1 singlet ground state and the first excited triplet state is rather different among these Pr-based superconductors, e.g., $\Gamma_4^{(2)}$ at $\Delta_{CEF} = 7$ K for $PrOs_4Sb_{12}$[13] and $\Gamma_4^{(1)}$ at $\Delta_{CEF} = 130$ K in $PrPt_4Ge_{12}$.[11,14] It is therefore of great interest to systematically compare the superconducting properties of these materials, which may help to elucidate their pairing mechanisms. Similar to $PrOs_4Sb_{12}$, previous studies on polycrystalline samples of $PrPt_4Ge_{12}$ showed controversial results. Measurements of the specific heat and muon-spin rotation (μSR) suggest the possible existence of point nodes in the superconducting gap;[12] zero-field μSR also provides evidence of time-reversal symmetry breaking below T_c,[15] similar to what was observed for $PrOs_4Sb_{12}$.[16] However, ^{73}Ge nuclear quadrupole resonance (NQR) experiments display a pronounced coherence peak in the spin-lattice relaxation rate $1/T_1$ at temperatures just below T_c, suggesting s-wave SC.[17] Very recently, a possible scenario of multiband SC was proposed for $PrPt_4Ge_{12}$ based on the analysis of the critical fields[18] as well as photoemission spectroscopy.[19] However, these experiments were performed on polycrystalline samples at relatively high temperatures and therefore could not make a clear assertion on the gap symmetry. The reasons underlying such discrepancies of the gap structure in $PrPt_4Ge_{12}$ are not yet clear, and further measurements, in particular those based on high-quality single crystals, are badly needed.

In this paper, we probe the superconducting gap symmetry of $PrPt_4Ge_{12}$ by measuring the London penetration depth $\Delta\lambda(T)$ and the specific heat $C_p(T)$ of high-quality single crystals. Precise measurements of the penetration depth changes at low temperatures show $\Delta\lambda \sim T^n$ with $n = 3.2 \pm 0.1$, indicating that $PrPt_4Ge_{12}$ is actually neither a simple BCS nor a simple nodal superconductor. A detailed analysis of the superfluid density $\rho_s(T)$, converted from $\lambda(T)$, and the electronic specific heat $C_e(T)$ provides strong evidence of two-band SC for $PrPt_4Ge_{12}$.

II. SAMPLE PREPARATIONS AND CHARACTERIZATIONS

High-quality single crystals of $PrPt_4Ge_{12}$ were synthesized by applying multistep thermal treatments. First, polycrystalline samples were prepared from the nominal compositions of Pr (Ames, 99.9%), Pt foil (Chempur, 99.9%), and Ge pieces (Chempur, 99.9999%) by arc melting on a copper hearth in a purified Ar atmosphere. The obtained buttons, subsequently enclosed in a glassy carbon crucible and a Ta container, were thermally treated in a sealed and evacuated silica tube at 800 °C for 120 h before quenching in cold water.

The so-obtained samples were characterized by x-ray powder diffraction (XRD) performed on a HUBER imaging plate Guinier camera (CuKα_1 radiation, 2θ interval of 3°–100°), which identified them as a single phase (filled skutterudite $LaFe_4P_{12}$ type, space group $Im\bar{3}$). From the differential scanning calorimetry (DSC) measurements it can be inferred that $PrPt_4Ge_{12}$ melts congruently but exists only in a narrow temperature range of 810–869 °C. Therefore, recrystallization heat treatment was chosen as a method to synthesize sizable single crystals of $PrPt_4Ge_{12}$.

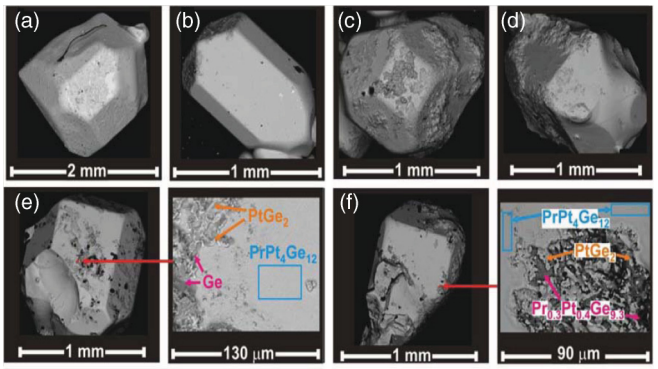

FIG. 1. (Color online) (a)–(f) Single crystals obtained from the samples after recrystallization heat treatment performed close to the melting point. For crystals (e) and (f), an enlarged fragment of their surfaces is shown, where the detected phases are indicated.

The $PrPt_4Ge_{12}$ samples were then powdered and sieved (40 μm mesh) and pressed into six pellets (diameter of 10 mm), which were placed into glassy carbon crucibles, welded into Ta containers, and sealed in evacuated silica tubes. To avoid possible contamination with oxygen, the above procedures were performed inside an argon-filled glove box. Further thermal treatment was performed at 867 °C for 60 days. The obtained crystals have a size up to 2 mm (see Fig. 1). A few crystals were powdered for XRD analysis. Phase analysis performed on the obtained powder pattern revealed the presence of two phases in the crystals: $PrPt_4Ge_{12}$ [a = 8.6105(2) Å, in good agreement with that reported before[11]] and the minority $PtGe_2$ phase. Multiphase Rietveld refinement showed that the filled skutterudite content is 98.5(5) wt. %. To clarify the phase distribution of the synthesized crystals, energy-dispersive x-ray spectroscopy (EDXS) on a Jeol JSM 6610 scanning electron microscope equipped with an UltraDry EDS detector (ThermoFisher NSS7 system) and an ESEM FEI Quanta 200 FEGi system (Genesis 2000 EDAX detector) was performed. The intensities of the lines GeK_α, PtL_β, and PrL_β were determined at an excitation current of 50 nA at 25 keV. The average compositions of the $PrPt_4Ge_{12}$ phase, obtained from three independent measurements for each of the crystals shown in Fig. 1, as well as other detected phases are listed in Table I. The compositions of the $PrPt_4Ge_{12}$ phase are very close to the 1:4:12 stoichiometry. Taking into account this fact as well as the refined unit-cell parameters, we conclude that all the crystals have a stoichiometric composition. As shown in Fig. 1, a small number of impurity phases, including the nonmagnetic, nonsuperconducting $PtGe_2$, free Ge, and a solid solution of Pr, Pt, and Ge with unknown physical properties, are located on the crystal surfaces. This can be best seen on crystal e [see Fig. 1(e)], which was broken off from a large piece. In the ternary phase diagram we observe an equilibrium only between $PrPt_4Ge_{12}$, $PtGe_2$, and Ge. No other ternary phases were detected in this region, and a small enlargement of the lattice parameter of Ge may indicate the solubility of other components in its lattice. It is noted that the Pr-containing additional phases on the surface may exhibit a pronounced upturn in the low-temperature specific-heat data, as previously seen in the polycrystalline samples.[12]

TABLE I. Phase compositions of the $PrPt_4Ge_{12}$ crystals shown in Fig. 1 from the EDXS analysis. The symbol A marks those black spots on the sample surfaces which indicate the glue from the pad.

Crystal	Composition	Phases on the surface
a	$Pr_{1.1(2)}Pt_{4.1(2)}Ge_{11.9(2)}$	$PtGe_2$, Ge, A
b	$Pr_{0.8(2)}Pt_{4.1(2)}Ge_{12.2(2)}$	$PtGe_2$, Ge, $Pr_{0.3}Pt_{0.3}Ge_{9.4}$, A
c	$Pr_{1.0(2)}Pt_{3.9(2)}Ge_{12.0(2)}$	$PtGe_2$, Ge, $Pr_{0.1}Pt_{0.4}Ge_{9.5}$, A
d	$Pr_{0.8(2)}Pt_{3.9(2)}Ge_{12.2(2)}$	$PtGe_2$, Ge
e	$Pr_{0.9(2)}Pt_{4.1(2)}Ge_{12.0(2)}$	$PtGe_2$, Ge, A
f	$Pr_{0.8(2)}Pt_{4.0(2)}Ge_{12.1(2)}$	$PtGe_2$,$Pr_{0.3}Pt_{0.4}Ge_{9.3}$

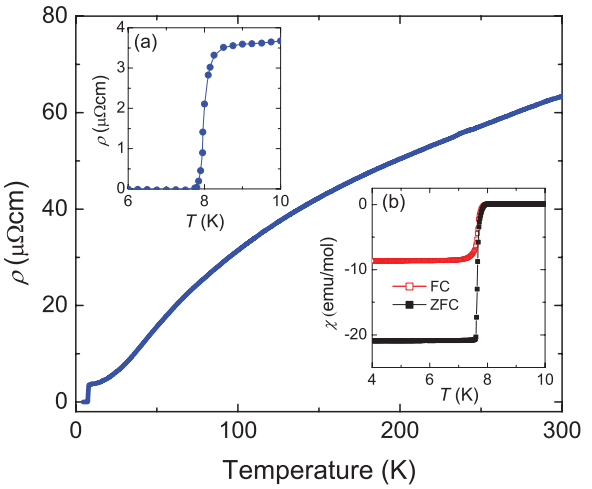

FIG. 2. (Color online) Temperature dependence of the electrical resistivity $\rho(T)$ for $PrPt_4Ge_{12}$. Insets (a) and (b) show the superconducting transitions in the electrical resistivity $\rho(T)$ and magnetic susceptibility $\chi(T)$, respectively.

In this context, we study the physical properties of $PrPt_4Ge_{12}$ by using the samples from the same batch as crystal a. In order to get rid of these surface contaminations, we have carefully polished the samples prior to the measurements, which enables us to probe the true behavior of $PrPt_4Ge_{12}$. The samples are characterized by measurements of electrical resistivity and magnetization. Figure 2 presents the electrical resistivity $\rho(T)$ for $PrPt_4Ge_{12}$, which shows an S-shape behavior upon cooling down from room temperature, as often observed in d-band materials. A sharp superconducting transition, evidenced from both the electrical resistivity $\rho(T)$ [inset (a)] and the magnetic susceptibility $\chi(T)$ [inset (b)], together with a large resistivity ratio [$\rho(300\ \mathrm{K})/\rho(8\ \mathrm{K}) = 19$] confirm the high quality of our single crystals. Furthermore, the superconducting transition temperatures T_c, determined from the zero resistivity and the onset of the magnetic susceptibility, are nearly the same ($T_c \simeq 7.8$ K), proving good homogeneity of the samples.

III. PENETRATION DEPTH AND SUPERFLUID DENSITY

Precise measurements of the resonant frequency shift $\Delta f(T)$ were performed by utilizing a tunnel diode oscillator (TDO) based self-inductance method at an operating frequency of 7 MHz down to about 0.5 K in a ^{3}He cryostat.[20] The change of the penetration depth is proportional to the resonant

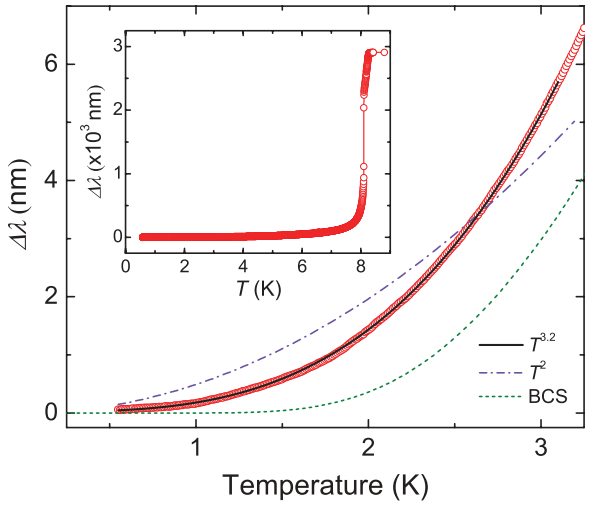

FIG. 3. (Color online) Temperature dependence of the penetration depth $\Delta\lambda(T)$ for $PrPt_4Ge_{12}$. Solid, dash-dotted, and dashed lines represent the fits of $\Delta\lambda \sim T^{3.2}$, $\Delta\lambda \sim T^2$ (point node), and the single-gap BCS model, respectively. The inset shows $\Delta\lambda(T)$ over the entire temperature range.

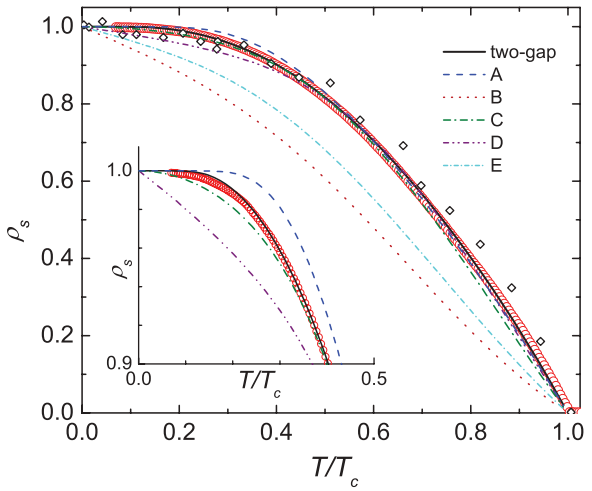

FIG. 4. (Color online) Superfluid density $\rho_s(T)$ vs normalized temperature T/T_c. The inset expands the low-temperature region. Circles and diamonds display the experimental data derived from TDO measurements (this study) and μSR experiments (from Ref. 12), respectively. Lines shows theoretical fits of various gap functions as listed in Table II.

frequency shift, i.e., $\Delta\lambda(T) = G\Delta f(T)$, where G is solely determined by the sample and coil geometries.[4] In this context, $\Delta\lambda(T)$ is extrapolated to zero at $T = 0$ by polynomial regression, i.e., $\Delta\lambda(T) = \lambda(T) - \lambda_0$. Here the value of zero-temperature penetration depth, $\lambda_0 = 114$ nm, was adopted from previous μSR experiments.[12]

The inset of Fig. 3 shows the change of the penetration depth $\Delta\lambda(T)$ up to 9 K, which reveals a sharp superconducting transition at $T_c \simeq 8.1$ K. Here $G = 2.13$ Å/Hz. It is noted that we have measured the penetration depth for several samples and the data are well reproducible. The values of T_c, derived for different samples by distinct methods, are nearly the same too. In the main plot of Fig. 3, we present $\Delta\lambda(T)$ at low temperatures, together with the fits of various models to the data. Obviously, the standard BCS model cannot describe the experimental data. Moreover, the penetration depth $\Delta\lambda(T)$ deviates also from that of nodal SC, for which a linear and quadratic temperature dependence is expected for the case of line and point nodes, respectively. Instead, a power law of $\Delta\lambda \sim T^n$ ($n = 3.2 \pm 0.1$) presents a reasonable fit to the experimental data. An enhanced power-law exponent n, e.g., a quadratic temperature dependence in d-wave superconductors, may arise from nonlocal effects or impurity scattering.[21] However, such possibilities are excluded for $PrPt_4Ge_{12}$ because both the penetration depth ($\lambda_0 = 114$ nm)[12] and the mean free path ($l = 103$ nm) are much larger than the coherence length ($\xi_0 = 13.5$ nm),[12] implying that the samples are in the clean and local limit. Here we estimate the mean free path from $l = [\frac{\xi_0^{-2} - 1.6\times10^{12}\rho_0\gamma_n T_c}{1.8\times10^{24}(\rho_0\gamma_n T_c)^2}]^{0.5}$,[22] where ρ_0, ξ_0, and γ_n represent the electrical resistivity at $T_c = 7.8$ K ($\rho_0 = 3.5 \times 10^{-6}$ Ω cm), the aforementioned coherence length, and the Sommerfeld coefficient at T_c ($\gamma_n = 1795$ erg cm^{-3} K^{-2}), respectively. On the other hand, multiband effects may also give rise to power-law-like behavior at low temperatures with a large exponent n, which will be further elucidated by the analysis of both the superfluid density and specific heat.

The superfluid density $\rho_s(T)$ provides an important characterization of the superconducting gap symmetry. Figure 4 shows the temperature dependence of the normalized superfluid density $\rho_s(T)$ for $PrPt_4Ge_{12}$ (circles), which is calculated by $\rho_s = [\lambda_0/\lambda(T)]^2$. For comparison, in Fig. 4 we also include the superfluid density from the μSR results determined on polycrystalline samples (diamonds).[12] Obviously, these two data sets are quite compatible, although the μSR data have a poor resolution when compared with the TDO results. Thus, the TDO data allow us to probe the gap structure of $PrPt_4Ge_{12}$ in a much more precise way than before.

The superfluid density can be calculated by

$$\rho_s(T) = 1 + 2\left\langle \int_0^\infty \frac{\partial f}{\partial E} \frac{E}{\sqrt{E^2 - \Delta_k^2(T)}} dE \right\rangle_{\mathrm{FS}}, \quad (1)$$

where $f = (e^{\sqrt{E^2+\Delta_k^2(T)}/k_BT} + 1)^{-1}$ is the Fermi distribution function and $\langle\cdots\rangle_{\mathrm{FS}}$ denotes the average over the Fermi surface. For the temperature dependence of the energy gap, we take $\Delta(T) = \Delta_0 \tanh\{\frac{\pi k_B T_c}{\Delta_0}[\frac{2}{3}\frac{\Delta C_e}{\gamma_n T_c}(\frac{T_c}{T} - 1)]^{0.5}\}$.[23] Here ΔC_e is the specific-heat jump at T_c. Note that Eq. (1) is applicable for various gap functions Δ_k [$= \Delta(\theta,\phi)$] in the pure/local limit. Given a gap function $\Delta(\theta,\phi)$, one can fit it to the experimental data. Here θ and ϕ denote the angles away from the z axis and x axis in k space, respectively. In this analysis, the zero-temperature gap amplitude Δ_0 is the sole fitting parameter.

Possible symmetries of the order parameter have been theoretically investigated for the skutterudite superconductors with tetrahedral point-group symmetry (T_h).[24] Various gap functions $\Delta(\theta,\phi)$, restrained by the crystal symmetry, have been adopted to fit the superfluid density $\rho_s(T)$ of $PrOs_4Sb_{12}$.[4] Following the methods used in Ref. 4, here we apply a similar analysis to the experimentally obtained $\rho_s(T)$ data of $PrPt_4Ge_{12}$. Figure 4 presents the fits of different gap functions allowed by the crystal symmetry; the derived fitting

TABLE II. Summary of various gap functions and so-derived fitting parameters Δ_0.

Model	Gap function $\Delta(\theta,\phi)$	Δ_0/k_BT_c
A	Δ_0	1.76
B	$\lvert\Delta_0 \sin\theta \sin\phi\rvert$	4.0
C	$\lvert\Delta_0 \sin\theta\rvert$	2.7
D	$\Delta_0(1-\sin^4\theta\cos^4\theta)$	2.9
E	$\Delta_0[1-(\sin^4\phi+\cos^4\phi)\sin^4\theta]$	3.2

parameters of Δ_0 are summarized in Table II. Apparently, the gap functions B and E cannot reproduce the experimental data. On the other hand, the fits of functions A, C, and D are close to the experimental data but show significant deviations at low temperatures (inset of Fig. 3). We note that models C and D, both having point nodes in the superconducting gap, were previously assumed to present a good fit to the μSR data,[15] which are rather scattered at low temperature. The more precise measurements of the penetration depth $\Delta\lambda(T)$ and the corresponding superfluid density $\rho_s(T)$ indicate that the conventional one-gap BCS model as well as the nodal-gap model D provide a poor fit to the low-temperature data. Nodal-gap model C can fit the TDO data relatively well, but significant deviations remain below $0.3T_c$. Instead, a two-gap model is capable of giving a much better fit to our experimental data.

In the case of two-band superconductors, the superfluid density can be extended to the following linear combination:[25]

$$\widetilde{\rho}_s(T) = x\rho_s\left(\Delta_0^1,T\right) + (1-x)\rho_s\left(\Delta_0^2,T\right), \qquad (2)$$

where Δ_0^i $(i=1,2)$ represent the size of two gaps at zero temperature and x is the relative weight of the contributions from Δ_0^1. For the simplest scenario (BCS SC), the two energy gaps are isotropic. As shown in Fig. 4, the two-gap BCS model nicely fits the experimental data of $PrPt_4Ge_{12}$ over the entire temperature region we measured. The so-derived parameters of $\Delta_0^1 = 0.8\,k_BT_c$, $\Delta_0^2 = 2.0\,k_BT_c$, and $x = 0.15$ meet the theoretical constraints that one gap is larger than the BCS value and the other one is smaller,[26] as demonstrated in the prototype two-gap BCS superconductor MgB_2.[25]

IV. SPECIFIC HEAT

The superconducting gap symmetry of $PrPt_4Ge_{12}$ is further characterized by measuring the heat capacity in a ^{3}He cryostat using a relaxation method. In Fig. 5, we present the low-temperature specific heat $C_p(T)$ of a polished $PrPt_4Ge_{12}$ single crystal. A sharp superconducting transition is observed at $T_c = 7.7$ K, being close to that determined from other experiments on this crystal. The specific-heat data above T_c can be fitted by a polynomial expansion $C_p(T) = \gamma_nT + \beta T^3$. Here $C_e = \gamma_nT$ and $C_{ph} = \beta T^3$ denote the electronic and phonon contributions, respectively. This yields the Sommerfeld coefficient in the normal state, $\gamma_n = 69$ mJ/mol K^2, and the Debye temperature $\Theta_D = 190$ K, which are close to those found in the case of polycrystalline samples.[12] For polycrystals,[12] a pronounced upturn was previously reported in the low-temperature specific heat $C_e(T)/T$. Similar specific-heat anomalies were also observed in some as-grown single

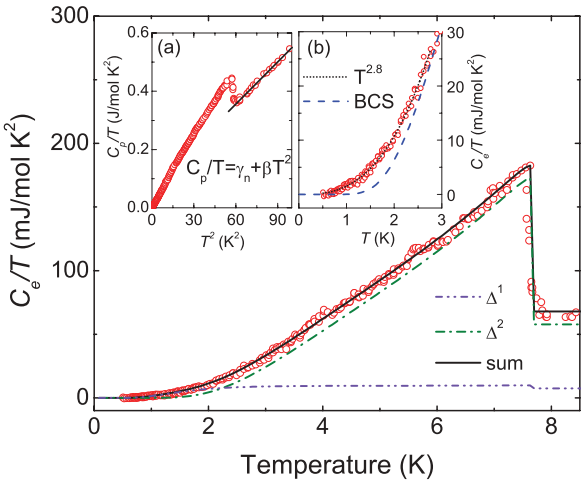

FIG. 5. (Color online) Temperature dependence of the electronic specific heat $C_e(T)/T$ of a $PrPt_4Ge_{12}$ single crystal at zero field. Dash-dotted lines (green and blue) and the solid line show the individual and total contributions of the two gaps to the specific heat $C_e(T)/T$, respectively. Inset (a) shows the total specific heat, $C_p(T)/T$, plotted as a function of T^2. Inset (b) shows the electronic specific heat $C_e(T)/T$ at low temperatures, fitted by $C_e/T \sim T^{2.8}$ (dotted line). The dashed line refers to the standard BCS model.

crystals. A careful examination showed that such an upturn in $C_e(T)/T$ has to be attributed to a nuclear Schottky anomaly caused by the Pr-containing surface contaminations. Indeed, the specific-heat anomaly disappears for the polished single crystal, as shown in Fig. 5, allowing us to accurately analyze its low-temperature behavior.

The electronic specific heat of $PrPt_4Ge_{12}$, obtained after subtracting the phonon contributions, is presented in the main part and inset (b) of Fig. 5 as C_e/T vs T, together with the fits of various models. As shown in inset (b), the data can be well described by a power law, $C_e/T \sim T^{2.8}$. This behavior deviates from the quadratic temperature dependence of $C_e(T)/T$ reported in Ref. 12. The discrepancy is likely to result from the nuclear Schottky anomaly of the polycrystalline samples discussed before. With the previous data,[12] a proper subtraction of this Schottky anomaly is difficult, and therefore, deviations from the true specific-heat behavior become likely at low temperatures. Furthermore, the standard BCS model is not sufficient to fit the experimental data [Fig. 5(b)], while the two-gap BCS model presents the best fit to the $C_e(T)/T$ data (main figure). According to the phenomenological two-gap BCS model, the heat capacity is taken as the sum of contributions from the two bands, each one following the BCS-type temperature dependence.[27] In the main panel of Fig. 5, we plot the contributions from the two superconducting gaps, $\Delta_0^1 = 0.8k_BT_c$ and $\Delta_0^2 = 2.0\,k_BT_c$, as well as their sum (solid line). The weight contributed from the first gap, Δ_0^1, is $x = 0.12$. All these fitting parameters are remarkably consistent with those obtained from the superfluid density $\rho_s(T)$, providing strong evidence of two-gap SC for $PrPt_4Ge_{12}$. The small x suggests that superconductivity in $PrPt_4Ge_{12}$ is mainly carried by the band with a large energy gap. It is noted that one cannot yet exclude the possibility of a different gap structure for the small gap due to its low weight x.

V. DISCUSSION

Evidence of BCS-like SC, including the two-gap type, has been observed in several skutterudite compounds. For example, $PrRu_4Sb_{12}$,[8] $PrRu_4As_{12}$,[9] and their non-$4f$ counterparts[12] are believed to be s-wave superconductors. Recent measurements indicate that $PrOs_4Sb_{12}$ is an extreme two-band superconductor;[6,7] here energy nodes were assumed to exist in the small gap, and the isotropic large gap dominates the superconducting properties near T_c,[7] or when a sufficiently large magnetic field is applied.[28] Two-gap BCS SC was also proposed for both $PrRu_4Sb_{12}$ (Ref. 7) and $LaOs_4Sb_{12}$,[29] the latter one suggesting that $4f$ electrons are not the origin of multiband SC. In $PrPt_4Ge_{12}$, band structure calculations indicate only a minor contribution of the $4f$ electrons to the density of states at the Fermi energy, suggesting that the $4f$ electrons may not be playing a significant role on SC in this compound either.[11] Indeed, the thermodynamic properties and low-lying CEF scheme of $PrPt_4Ge_{12}$ are rather different from those of the heavy-fermion compound $PrOs_4Sb_{12}$ but resemble other skutterudite compounds.[8,9] Indications of two-gap SC for $PrPt_4Ge_{12}$ were also inferred from recent measurements of the upper and lower critical fields[18] and photoemission spectroscopy.[19] Furthermore, multiband SC is compatible with the observations of a coherence peak in the NQR measurements just below T_c.[17] Such a multigap structure seems to be characteristic for the skutterudite superconductors; the small gap, either with or without nodes, is rather subtle and can be easily destroyed by external effects, e.g., a magnetic field, so that the large gap is predominant. Recent μSR measurements performed on polycrystalline samples of $PrPt_4Ge_{12}$ showed evidence of time-reversal symmetry breaking.[15] To confirm it and check the possible existence of nodes in the small gap of $PrPt_4Ge_{12}$, it would be important to repeat the μSR measurements with high-quality single crystals and to measure the thermodynamic properties with high precision down to lower temperatures. Detailed calculations of its electronic structure are also highly desirable in order to further elucidate the multiband structure in $PrPt_4Ge_{12}$. Moreover, comparative studies of the Pr-based skutterudites and the non-f electron isostructural compounds, e.g., MPt_4Ge_{12} (M = Sr, Ba, and La), are necessary to reveal the potential role of f electrons on SC.

VI. CONCLUSION

In summary, we have studied the superconducting order parameter of $PrPt_4Ge_{12}$ by measuring the penetration depth $\Delta\lambda(T)$ and specific heat $C_p(T)$ on high-quality single crystals. For $T \ll T_c$, both quantities demonstrate a weak temperature dependence and can be fitted by a power-law behavior with a large exponent, i.e., $\Delta\lambda \sim T^{3.2}$ and $C_e/T \sim T^{2.8}$, which is inconsistent with both a single-gap BCS model and nodal-gap SC. Instead, we can describe the superfluid density $\rho_s(T)$ and the electronic specific heat $C_e(T)$ in terms of a phenomenological two-gap BCS model with consistent gap parameters of $\Delta_0^1 = 0.8\ k_BT_c$, $\Delta_0^2 = 2.0\ k_BT_c$, and $x = 0.12 \sim 0.15$, the weight contributed by the small gap. These findings have elucidated the controversial results found in the literature and provide strong evidence of multiband SC for $PrPt_4Ge_{12}$.

ACKNOWLEDGMENTS

We are grateful to E. Rosseeva, Y. Kohama, and C. T. van Degrift for providing experimental assistance. This work was supported by the National Basic Research Program of China (Grants No. 2009CB929104 and No. 2011CBA00103), the NSFC (Grants No. 10934005 and No. 11174245), the Zhejiang Provincial Natural Science Foundation of China, the Fundamental Research Funds for the Central Universities, and the Max Planck Society under the auspices of the Max Planck Partner Group of the MPI for Chemical Physics of Solids, Dresden, Germany.

*hqyuan@zju.edu.cn

[1] B. C. Sales, in *Handbook on the Physics and Chemistry of Rare Earths*, edited by K. A. Gschneidner, Jr., J.-C. G. Bünzli, and V. K. Pecharsky (Elsevier, Amsterdam, 2003), Vol. 33, p. 1.
[2] E. D. Bauer, N. A. Frederick, P.-C. Ho, V. S. Zapf, and M. B. Maple, Phys. Rev. B **65**, 100506(R) (2002).
[3] K. Izawa, Y. Nakajima, J. Goryo, Y. Matsuda, S. Osaki, H. Sugawara, H. Sato, P. Thalmeier, and K. Maki, Phys. Rev. Lett. **90**, 117001 (2003).
[4] E. E. M. Chia, M. B. Salamon, H. Sugawara, and H. Sato, Phys. Rev. Lett. **91**, 247003 (2003), and references therein.
[5] D. E. MacLaughlin, J. E. Sonier, R. H. Heffner, O. O. Bernal, B. L. Young, M. S. Rose, G. D. Morris, E. D. Bauer, T. D. Do, and M. B. Maple, Phys. Rev. Lett. **89**, 157001 (2002).
[6] G. Seyfarth, J. P. Brison, M.-A. Méasson, D. Braithwaite, G. Lapertot, and J. Flouquet, Phys. Rev. Lett. **97**, 236403 (2006).
[7] R. W. Hill, S. Y. Li, M. B. Maple, and L. Taillefer, Phys. Rev. Lett. **101**, 237005 (2008).
[8] N. Takeda and M. Ishikawa, J. Phys. Soc. Jpn. **69**, 868 (2000).
[9] T. Namiki, Y. Aoki, H. Sato, C. Sekine, I. Shirotani, T. D. Matsuda, Y. Haga, and T. Yagi, J. Phys. Soc. Jpn. **76**, 093704 (2007).
[10] E. Bauer *et al.*, Phys. Rev. Lett. **99**, 217001 (2007).
[11] R. Gumeniuk, W. Schnelle, H. Rosner, M. Nicklas, A. Leithe-Jasper, and Y. Grin, Phys. Rev. Lett. **100**, 017002 (2008).
[12] A. Maisuradze, M. Nicklas, R. Gumeniuk, C. Baines, W. Schnelle, H. Rosner, A. Leithe-Jasper, Y. Grin, and R. Khasanov, Phys. Rev. Lett. **103**, 147002 (2009).
[13] M. B. Maple, N. A. Frederick, P.-C. Ho, W. M. Yuhasz, and T. Yanagisawa, J. Supercond. Novel Magn. **19**, 299 (2006).
[14] M. Toda, H. Sugawara, K. Magishi, T. Saito, K. Koyama, Y. Aoki, and H. Sato, J. Phys. Soc. Jpn. **77**, 124702 (2008).
[15] A. Maisuradze, W. Schnelle, R. Khasanov, R. Gumeniuk, M. Nicklas, H. Rosner, A. Leithe-Jasper, Y. Grin, A. Amato, and P. Thalmeier, Phys. Rev. B **82**, 024524 (2010).
[16] Y. Aoki *et al.*, Phys. Rev. Lett. **91**, 067003 (2003).
[17] F. Kanetake, H. Mukuda, Y. Kitaoka, K. Magishi, H. Sugawara, K. M. Itoh, and E. E. Haller, J. Phys. Soc. Jpn. **79**, 063702 (2010).

[18]L. S. Sharath Chandra, M. K. Chattopadhyay, and S. B. Roy, Phil. Mag. **92**, 3866 (2012).
[19]Y. Nakamura, H. Okazaki, R. Yoshida, T. Wakita, H. Takeya, K. Hirata, M. Hirai, Y. Muraoka, and T. Yokoya, Phys. Rev. B **86**, 014521 (2012).
[20]C. T. Van Degrift, Rev. Sci. Instrum. **46**, 599 (1975).
[21]P. J. Hirschfeld and N. Goldenfeld, Phys. Rev. B **48**, 4219 (1993).
[22]T. P. Orlando, E. J. McNiff, Jr., S. Foner and M. R. Beasley, Phys. Rev. B **19**, 4545 (1979).
[23]R. Prozorov and R. W. Giannetta, Supercond. Sci. Technol. **19**, R41 (2006).
[24]I. A. Sergienko and S. H. Curnoe, Phys. Rev. B **70**, 144522 (2004).
[25]F. Manzano, A. Carrington, N. E. Hussey, S. Lee, A. Yamamoto, and S. Tajima, Phys. Rev. Lett. **88**, 047002 (2002).
[26]V. Z. Kresin and S. A. Wolf, Phys. C **169**, 476 (1990).
[27]F. Bouquet, Y. Wang, R. A. Fisher, D. G. Hinks, J. D. Jorgensen, A. Junod, and N. E. Phillips, Europhys. Lett. **56**, 856 (2001).
[28]L. Shu, D. E. MacLaughlin, W. P. Beyermann, R. H. Heffner, G. D. Morris, O. O. Bernal, F. D. Callaghan, J. E. Sonier, W. M. Yuhasz, N. A. Frederick, and M. B. Maple, Phys. Rev. B **79**, 174511 (2009).
[29]X. Y. Tee, H. G. Luo, T. Xiang, D. Vandervelde, M. B. Salamon, H. Sugawara, H. Sato, C. Panagopoulos, and E. E. M. Chia, Phys. Rev. B **86**, 064518 (2012).